

一种全桥 LLC 软开关焊接电源

陈延明¹, 王会雄¹, 王振民², 薛家祥², 李国进¹

(1. 广西大学 电气工程学院, 南宁 530004; 2. 华南理工大学 机械工程学院, 广州 510640)

摘 要: 采用变压器的励磁电感、隔直电容、变压器的漏电感和绕制的附加电感构成全桥 LLC 变换电路, 实现一种平特性的软开关全桥焊接电源。结果表明, 在整个负载工作范围内, 电路工作在两个谐振频率之间, 功率开关实现零电压开通, 整流二极管的实现零电流关断; 整个电路可以工作在更高的开关频率, 功率密度高, 损耗小, 效率高, 特别适合在大功率场合。文中讨论了其工作原理, 制作 3.2 kW 焊接电源, 并给出试验结果。

关键词: 焊接电源; LLC 全桥变换器; 谐振; 零电压开通; 零电流关断

中图分类号: TM 461.5 文献标识码: A 文章编号: 0253-360X(2014)05-0009-04

0 序 言

LLC 软开关变换电路, 软开关工作范围大, 开关频率高, 开关损耗小, 功率密度高, 动态响应能力好^[1-8], 可望成为新一代焊接电源的优选电路拓扑, LLC 软开关变换电路的平特性输出特别适合气体保护焊接电源, 稍加改进也可以应用在其它外特性的焊接电源中。

在输出功率较大场合, 需要采用 LLC 全桥变换电路, 由于电路开关频率高, 需要采用场效应管 (MOSFET) 作为功率开关, 可以采用场效应管并联的方法增加功率容量, 但场效应管一般耐压为 600 V 左右, 如果焊接电源的前级电路采用三相六开关升压型功率因数校正电路, 其输出电压一般为 750 V 左右, 采用场效应管作为功率开关耐压不够, 如果采用 IGBT 作为功率开关, 其耐压足够, 但开关频率过低, LLC 变换电路的优点又不能充分发挥。

为了进一步提高软开关大功率焊接电源的可靠性和效率, 文中采用全桥 LLC 变换器, 采用场效应管并联的方法实现软开关焊接电源, 其前级功率因数校正电路采用降压型的 PWM 整流器实现, PWM 整流器输出电压为 410 V, 使得全桥 LLC 变换器可以采用场效应管作为功率开关, 同时, 通过对 LLC 电路的直流增益和谐振槽的阻抗特性进行分析, 确立 LLC 全桥谐振电路的参数 (励磁电感、漏感、隔直电容等), 并制作了一台制作 3.2 kW 输出平特性的三相焊接电源, 其工作频率从 80 kHz 到 240 kHz, 并

给出试验结果。

1 电路工作原理

主电路如图 1 所示, 其中, 全桥变换电路的功率开关 VT₁ 与 VT₄ 同时导通同时关断; 功率开关 VT₂ 与 VT₃ 同时导通同时关断; VT₁ 与 VT₂ 驱动信号互补, 并有合适的死区时间; 同样, VT₃ 与 VT₄ 驱动信号互补, 并有合适的死区时间; 所有功率开关的驱动信号是占空比固定, 略小于 50%, 通过调节频率来调节输出电压。电感 L_r、电容 C_r 和变压器励磁电感 L_m 构成 LLC 谐振网络, 励磁电感参与部分阶段的谐振, 在 LLC 谐振变换器中有两个谐振频率, 将 L_r、C_r 振荡电路的谐振频率定义为

$$f_r = 1/2\pi \sqrt{L_r C_r} \quad (1)$$

将 L_r、L_m、C_r 的谐振频率定义为

$$f_m = 1/2\pi \sqrt{(L_m + L_r) C_r} \quad (2)$$

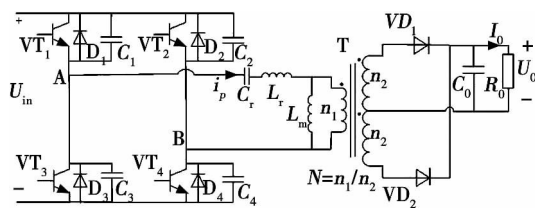


图 1 LLC 全桥主电路拓扑

Fig. 1 LLC full-bridge topology

整流电路由变压器 T、整流二极管、输出电容 C₀ 和负载构成, LLC 变换电路在工作频率大于 f_m 而小于 f_r, 由于谐振槽阻抗呈感性, 所以功率开关可以实

收稿日期: 2013-04-10

基金项目: 国家自然科学基金资助项目 (50567001); 南宁市科技攻关与新产品试制项目 (201102096G)

现零电压开通;同时,由于谐振槽电流由励磁电流和负载电流构成,当谐振槽电流等于励磁电流时,负载电流为零,整流二极管可以实现零电流关断。

图2为 LLC 电路工作时的基本波形,可将一个周期工作过程分为6个模式,如图3所示,图3中实线表示电流流通的路径,其中 $C_1 = C_2 = C_3 = C_4$, n_1 为变压器原边绕组匝数, n_2 为副边绕组匝数, N 为变压器匝比 n_1/n_2 。

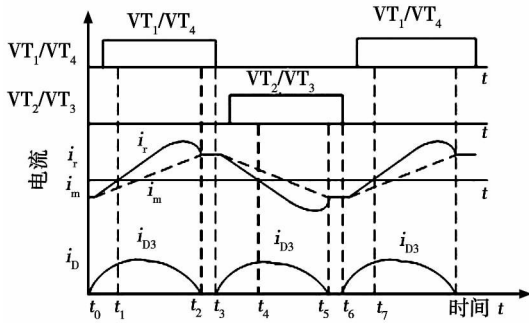


图2 主电路开关管驱动信号时序图

Fig. 2 Driving signal sequence and current waveforms

1.1 开关模式1($t_0 \sim t_1$)

t_0 时刻,所有开关管处于关断状态,谐振槽电流对电容 C_1, C_4 放电,对电容 C_2, C_3 充电,当电容 C_1, C_4 放电到零,二极管 D_1, D_4 导通,开关管 VT_1, VT_4 的漏源极电压被箝位为零, VT_1, VT_4 可实现零电压开通。此模式中,只有 L_r, C_r 参与谐振,励磁电感 L_m 电压上正下负,副边整流二极管 VD_1 导通,励磁电感 L_m 被输出电压箝位为 nU_0 , L_m 上的电流从负方向线性上升,励磁电感能量回馈到电源。

1.2 开关模式2($t_1 \sim t_2$)

t_1 时刻,开关管 VT_1, VT_4 和二极管 VD_1 导通,谐振槽电流换向,励磁电感 L_m 继续被输出电压箝位为 nU_0 , L_m 上的电流线性上升,变压器原边、副边进行能量传递。 t_2 时刻,当谐振槽电流 i_r 与励磁电流 i_m 相等,变压器的副边电流为零,二极管 VD_1 实现零电流关断。此模式中,只有 L_r, C_r 参与谐振。

1.3 开关模式3($t_2 \sim t_3$)

变压器副边电流降为零后,变压器原边、副边断开,没有电磁联系,在此模式中, L_r, C_r, L_m 均参与电路谐振,由于励磁电感大,谐振周期变长,如果 L_m 远大于 L_r ,电流可以认为是恒流,至 VT_1, VT_4 关断时,此阶段结束。

到此,半周期的工作状态结束,开关模式4~6是另外半周的工作情况,其工作状态与模式1~3相似,在此不再详述。

由 LLC 变换电路工作模式可知,在轻载时,由

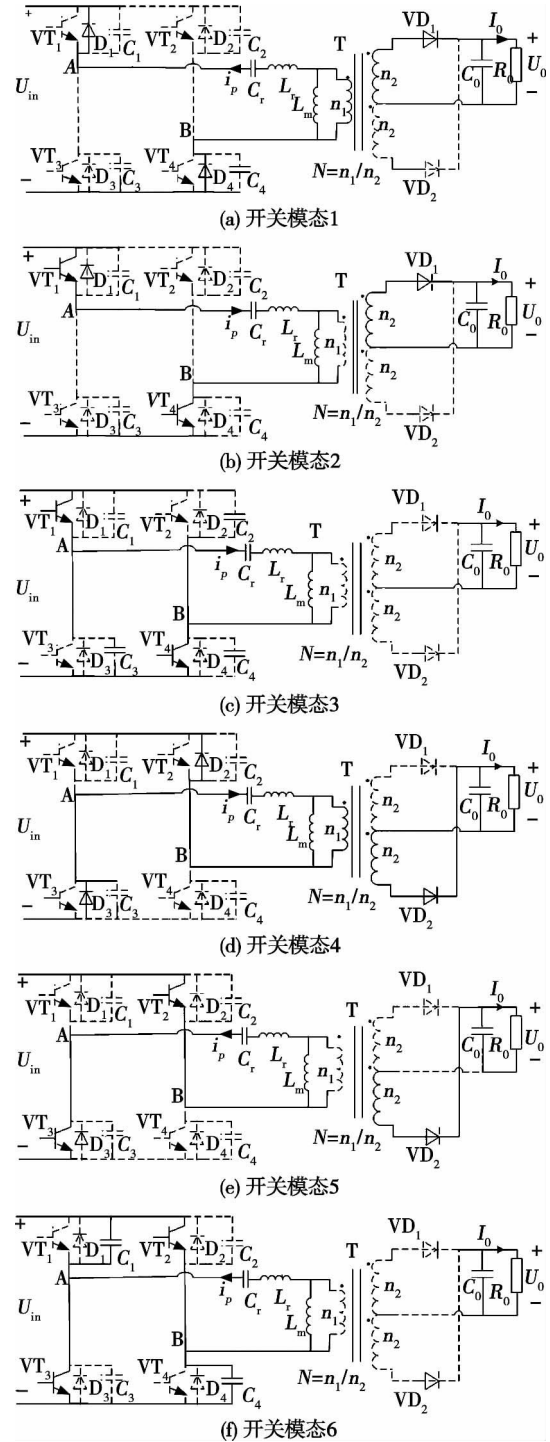


图3 各个工作模式等效电路图

Fig. 3 Equivalent circuit of each operating mode

于存在励磁电流,其功率开关可以实现零电压开通;重载时,只要工作区间落在 $f_m \sim f_r$ 之间,当谐振槽电流与励磁电流相等时,变压器的副边无电流,整流二极管可实现零电流关断。

2 电路参数的设计

图4为 LLC 全桥谐振变换器交流等效电路,利

用基波分析法^[8]将焊接时的电弧电压、电流所等效的负载折算到原边,可得到等效负载 R_{ac} 为

$$R_{ac} = 8N^2 R_L / \pi^2 \quad (3)$$

式中: N 为变压器变比; R_L 为负载.

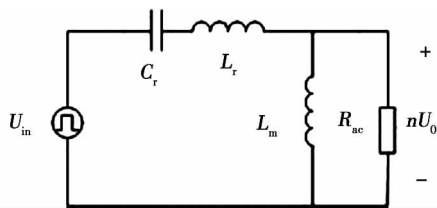


图4 LLC 谐振变换器交流等效电路

Fig. 4 Equivalent circuit of full-bridge LLC converter

从 LLC 变换电路的基波等效电路可以得出电压增益为

$$M_{dc} = \frac{U_0}{U_{in}} = \frac{1}{n} \frac{1}{\sqrt{\left(1 + \frac{1}{k} - \frac{1}{kf_n^2}\right)^2 + \left(f_n - \frac{1}{f_n}\right)^2 Q^2}} \quad (4)$$

式中: $f_n = f_s / f_r$ 为归一化频率; f_s 为开关频率; Q 为电路品质因数; $K = L_m / L_r$ 为励磁电感与谐振电感比值, 谐振槽的阻抗特性为

$$Z_{in} = \left[\frac{k^2 f_n^2 Q}{1 + k^2 f_n^2 Q} + j \left(f_n - \frac{1}{f_n} + \frac{k f_n}{1 + k^2 f_n^2 Q} \right) \right] Q \quad (5)$$

对于不同 K 和 Q 值的组合, 可以获得不同的增益曲线, 如图 5 所示.

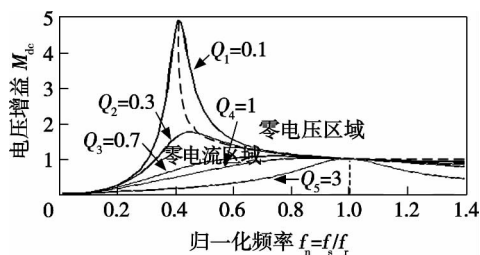


图5 LLC 谐振槽电压增益曲线

Fig. 5 Gain characteristic for full-bridge LLC converter

由图 5 可见 K 和 Q 的值越小, 最大电压增益越大, 变换器可实现较宽范围电压输入, 由于变换器前级是功率因数校正电路, 其输出电压基本恒定, 给 K 和 Q 值提供便利; K 值减小, 则励磁电感 L_m 的值减小, 使得励磁电感的峰值电流和谐振槽的电流有效值 I_{RMS} 增大, 原边开关管的关断电流增大, 损耗增加. 试验结果表明 K 值大于 6 时, LLC 电路易于设计; 同时, 保证电路工作在两个谐振频率之间时, 谐振槽的增益大于 1, 易于实现零电压开关, 在实际设

计时, 根据这些情况进行相关参数的选择.

3 试验结果

在实验室构建一台三相输入, 输出为平特性的焊接电源. 采用降压型 PWM 整流器实现功率因数校正, 其输出电压为 410 V, 采用并联的 MOSFET 作为 LLC 变换电路的功率开关.

所研制三相交流输入气体保护焊机功率为 3.2 kW, 采用降压型整流电路后, 焊接电源的输入电压为 410 V, 输出为 32 V, 输出电流为 100 A, 工作频率从 80 ~ 240 kHz. 主电路功率管选用 MOSFET 并联. 通过计算, 变压器匝比为 13, 电感 L_m 、 L_r 比为 8, 电路品质因数为 0.66, 励磁电感为 155.2 μ H, 谐振电感为 19.4 μ H, 谐振电容为 22.7 nF, 驱动信号占空比设置为 48%, 留有一定的死区时间. 焊接电源动态特性由电压调节器决定, 焊接电源的输出电压和给定电压比较, 误差信号经过电压调节器处理, 其输出经过压控振荡器转换成频率信号, 控制功率开关的通断, 电压调节器的参数根据气体保护焊的工艺特性进行适当的设置.

图 6a、b 分别为空载和满载时, LLC 变换器的主要波形, U_0 为输出电压, i_r 为谐振槽电流, U_1 、 U_2 分别为开关管 VT₁/VT₄ 和 VT₂/VT₃ 驱动信号. 由图 6

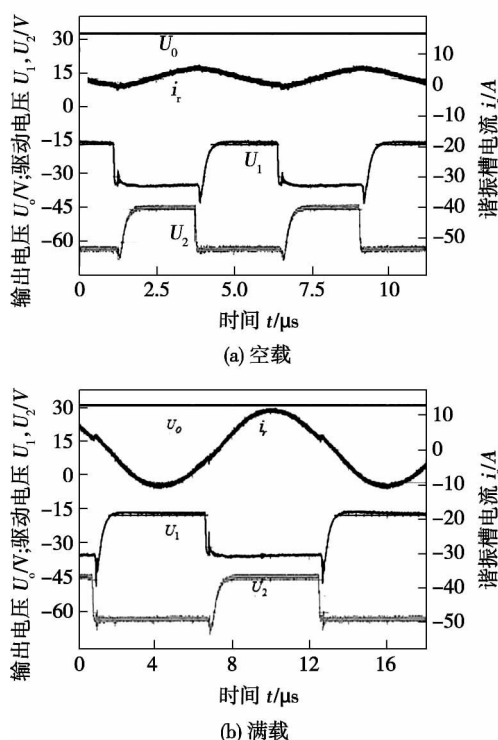


图6 空载和满载时谐振槽的典型波形

Fig. 6 Typical waveforms of resonant tank under no-load and full-load condition

可见,空载时,由于负载电流基本为零,谐振槽电流与励磁电感电流波形一致,近似为三角波,是输出电压的原边折算值对励磁电感充、放电;满载时,由于谐振,其谐振槽电流近似为正弦波。图 7 的效率比较显示 LLC 电源效率比移相全桥开关电源高。

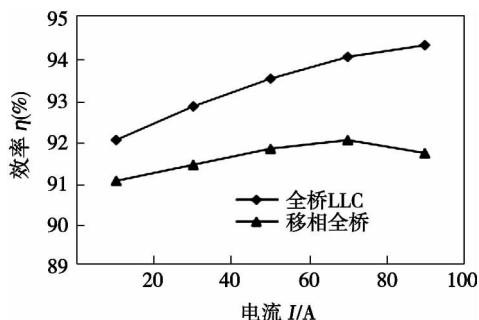


图 7 LLC 变换器和移相全桥变换器的效率比较

Fig. 7 Efficiency of LLC converter phase-shift FB converter

4 结 论

(1) 所研制的全桥 LLC 焊接电源,在整个负载范围内实现软开关,其中原边电路实现零电压开通,通过选择合适的励磁电感降低其关断损耗;副边整流二极管可以实现零电流关断。

(2) 整个电路功耗小,效率比现有的移相全桥开关电源高,特别适合输出平特性的气体保护焊机,稍加改进,也可以推广到其它输出特性的大功率焊接电源。

参考文献:

[1] Lee Junyoung, Jeong Yuseok, Han Byungmoon. An isolated DC/

DC converter using high-frequency unregulated LLC resonant converter for fuel cell applications [J]. IEEE Transactions on Industrial Electronics, 2011, 58(7): 2926–2934.

- [2] Yang Bo. Topology investigation for front end DC/DC power conversion for distributed power system [D]. Virginia: Virginia Polytechnic Institute and State University, 2003.
- [3] Lu Bing. Investigation of high density integrated solution for AC/DC conversion of a distributed power system [D]. Virginia: Virginia Polytechnic Institute and State University, 2006.
- [4] Feng W, Lee F C, Mattavelli P. Simplified optimal trajectory control (SOTC) for LLC resonant converters [J]. IEEE Transactions on Power Electronics, 2013, 28(5): 2415–2426.
- [5] Feng W, Lee F C, Mattavelli P. Optimal trajectory control of burst mode for LLC resonant converter [J]. IEEE Transactions on Power Electronics, 2013, 28(1): 457–466.
- [6] 朱志明,赵 港,陈 杰,等. 全负载范围零压零流软开关焊接逆变电源 [J]. 焊接学报, 2009, 30(2): 9–12.
Zhu Zhiming, Zhao Gang, Chen Jie, et al. Full-load range zero-voltage zero-current soft-switching inverter arc welding power supply [J]. Transactions of the China Welding Institution, 2009, 30(2): 9–12.
- [7] 王瑞超,薛家祥. 软开关弧焊逆变电源的动特性分析 [J]. 焊接学报, 2012, 33(10): 17–20.
Wang Ruichao, Xue Jiaxiang. Analysis for dynamic characteristics of soft-switch arc welding inverter [J]. Transactions of the China Welding Institution, 2012, 33(10): 17–20.
- [8] 王瑞超,薛家祥. 软开关弧焊逆变电源外特性的理论分析 [J]. 焊接学报, 2012, 33(4): 29–32.
Wang Ruichao, Xue Jiaxiang. Theoretical analysis for output characteristics of soft-switching arc welding inverter [J]. Transactions of the China Welding Institution, 2012, 33(4): 29–32.

作者简介: 陈延明,男,1966 年出生,博士,教授,博士研究生导师。主要研究方向为电力电子应用,焊接电源等。发表论文 20 余篇。
Email: yanmingchen@126.com

通讯作者: 李国进,男,博士,高级工程师。Email: lgjx@163.com

MAIN TOPICS ,ABSTRACTS & KEY WORDS

Comparison and analysis on dissimilar metals welding of aluminum alloy to galvanized steel by different welding-brazing methods

SHI Yu¹, HE Cuicui¹, HUANG Jiankang¹, CAO Rui¹, YU Shurong² (1. State Key Laboratory of Advanced Processing and Recycling of Nonferrous Metals, Lanzhou University of Technology, Lanzhou 730050, China; 2. School of Mechanical and Electrical Engineering, Lanzhou University of Technology, Lanzhou 730050, China) . pp 1 - 4

Abstract: The welding-brazing lap joints of aluminum / galvanized steel were obtained by using the pulse bypass coupling arc MIG welding (Pulsed DE-GMAW), cold metal transfer (CMT) and laser welding, respectively. The analysis on the microstructure, shape and elements of welding joint shows that these three welding methods are feasible for welding aluminum to steel, due to the low welding heat input of these methods, good weld formation can be also obtained. In addition, the mechanical properties of weld bead are measured. The results show that the tensile-shear strength of lap joint can reached 80% of the tensile strength of aluminum alloy; the sample fracture in the heat affected zone of aluminum alloy. When the heat-input and welding parameters were appropriated, it can generate a thin layer of Al-Fe intermetallic compounds on the lap joint interface under these three methods, and the average thickness of the compound layer is about 8 μm , it is confirmed that the intermetallic compounds is composed of Fe_2Al_3 and FeAl_3 . The key of welding aluminum to steel is control the formation of intermetallic compound in the interface by reducing the heat input.

Key words: dissimilar metals welding of aluminum/steel; welding-brazing; microstructure structure; intermetallic compounds

Interfacial behavior and joint strength of Ti(C ,N) and 40Cr joints obtained by liquid-solid diffusion hybrid bonding method

WU Mingfang, KUANG Hongjin, WANG Fei, XU Guoxiang (Provincial Key Laboratory of Advanced Welding Technology, Jiangsu University of Science and Technology, Zhenjiang 212003, China) . pp 5 - 8

Abstract: By presetting asymmetric Ti/Cu interlayer, liquid-solid diffusion bonding of Ti(C ,N) -based cermet and 40Cr was performed. The interfacial microstructure, joint strength and their effect factor were investigated. The results showed that, through presetting asymmetric Ti/Cu interlayer, the metallurgical bondings between Ti(C ,N) -based cermet and Cu foil and between Cu foil and 40Cr steel can be achieved in liquid-solid diffusion welding, respectively. The phase at the interface of Ti(C ,N) -based cermet has gradient distribution, forming Ti(C ,N) -based cermet/ TiAl_2 / Ti_2Cu / TiCu /Cu foil structure. There exists large welding residual tensile stress and brittle TiAl_2 intermetallic compounds in the interface zone close to Ti(C ,N) based cermet, being the key factor of restricting the strength of

welded joint. By only using Cu foil as interlayer, it is difficult to join Ti(C ,N) based cermet to Cu foil effectively in solid diffusion welding of Ti(C ,N) based cermet even at the heating temperature of 1 223 K and the pressure of 20 MPa.

Key words: Ti(C ,N) based cermet; 40Cr steel; liquid-solid diffusion hybrid bonding; interfacial microstructure; joint strength

A full-bridge LLC soft-switching welding power supply

CHEN Yanming¹, WANG Huixiong¹, WANG Zhenmin², XUE Jiangxiang², LI Guojin¹ (1. College of Electrical Engineering, Guangxi University, Nanning 530004, China; 2. College of Mechanical Engineering, South China University of Technology, Guangzhou 510640, China) . pp 9 - 12

Abstract: By utilizing the transformer magnetizing inductor, DC block capacitor, leakage inductance and the auxiliary inductor, a full-bridge LLC soft-switching welding power supply with constant output voltage was proposed. Because the converter was operated between the two resonant frequency in the whole load range, the zero voltage switching(ZVS) turn-on can be achieved for primary side power switch, and the zero current switching(ZCS) turn-off can be achieved for secondary rectifier diodes. The converter can be operated in higher frequency, with high density, lower losses and high efficiency, hence it is especially suitable for the high power applications. Moreover, the operation principles were discussed as well. Finally, a 3.2 kW welding power supply prototype had been implemented, and the experimental results were also presented.

Key words: welding power supply; LLC full-bridge converter; resonant; ZVS turn-on; ZCS turn-off

Flux-cored wire for underwater wet welding

GUO Ning^{1,2}, WANG Meirong², GUO Wei², FENG Jicai^{1,2} (1. State Key Laboratory of Advanced Welding and Joining, Harbin Institute of Technology, Harbin 150001, China; 2. Shandong Provincial Key Laboratory of Special Welding Technology, Harbin Institute of Technology at Weihai, Weihai 264209, China) . pp 13 - 16

Abstract: A novel flux-cored wire for underwater wet welding was developed. The underwater wet welding experiments with the water depth of 30 m were carried out by using a simulated pressure vessel and automatic welding machine. The experimental results show that welding process was stable and the good weld appearance could be obtained. According to the ANSI/AWS D3.6 1999, the tensile strength, bending property, hardness and impact toughness of the joint were studied. The results indicated that the fracture location of tensile test was in base material, no fracture was occurred during bending test and the acceptable impact toughness of joints about 30.25 J/cm² at 0 $^{\circ}\text{C}$ were also obtained. So the novel flux-cored wire could reach the